

Expanded View Figures

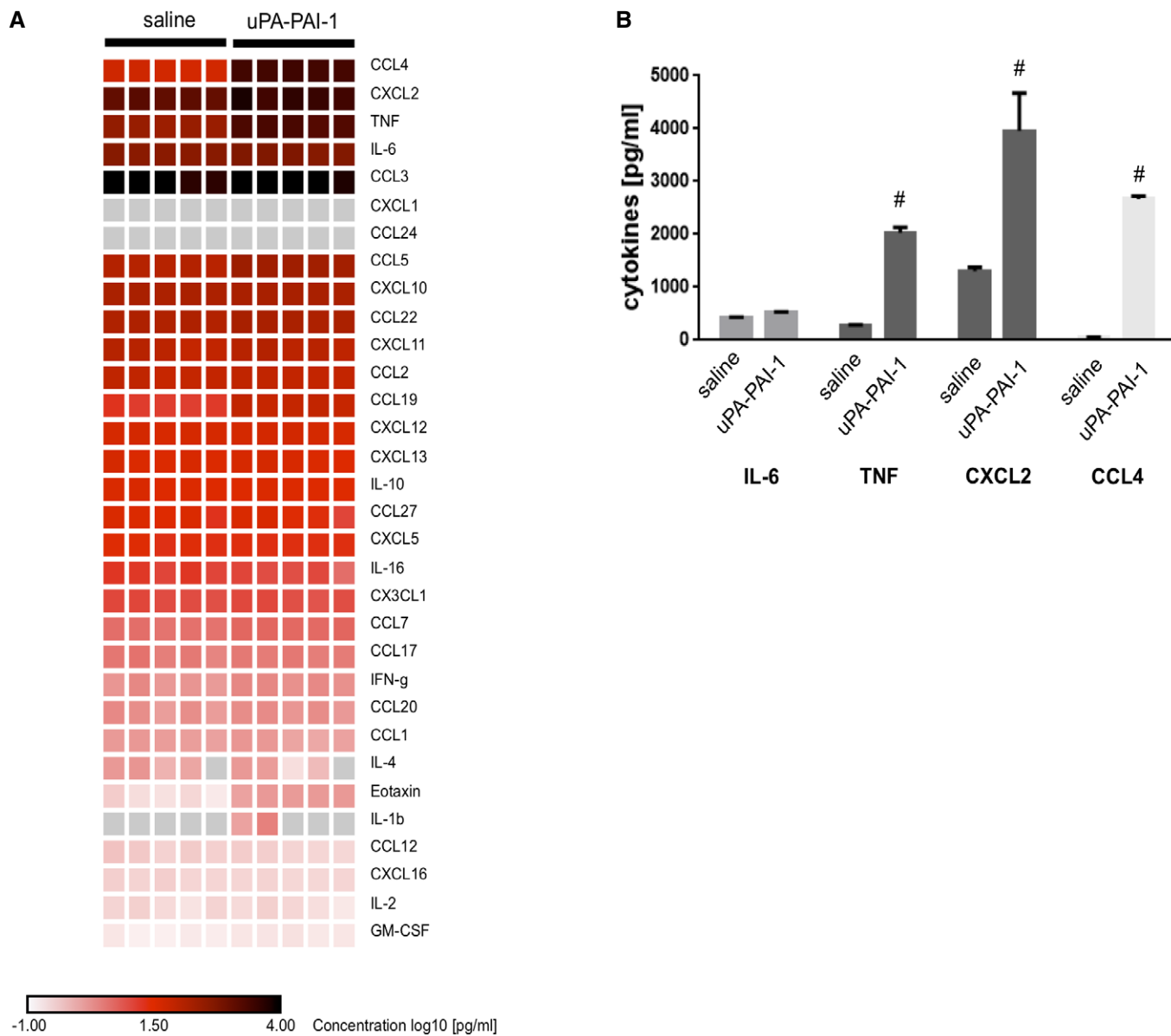


Figure EV1. Effect of uPA-PAI-1 heteromers on cytokine production in macrophages.

A Production of different cytokines by mouse RAW macrophages upon exposure to recombinant murine uPA-PAI-1 heteromers or saline as assessed by multiplex ELISA, results are shown as heatmap.

B In addition, quantitative data are provided for the most abundantly produced cytokines (mean ± SEM for *n* = 5 experiments per group; [#]*P* < 0.05 vs. saline; *t*-test).

Figure EV2. Molecular mechanisms underlying uPA-PAI-1-dependent neutrophil and cMO trafficking.

- A, B uPA-PAI-1-elicited recruitment of neutrophils (N) and classical monocytes (cMOs) to the peritoneal cavity of WT mice treated with anti-LFA-1/CD11a, anti-Mac-1/CD11b, anti-VLA-4/CD49d, anti-ICAM-1/CD54, anti-VCAM-1/CD106 mABs (A), anti-VLDLr mABs, anti-LRP-1 Abs, the MAPK inhibitors FR180204 (ERK1/2), SB202580 (p38), SP600125 (JNK) (B), or isotype control antibodies/drug vehicle as assessed by multi-channel flow cytometry, quantitative data are shown (mean \pm SEM for $n = 4-6$ mice per group; $^{\#}P < 0.05$ vs. saline; $^{*}P < 0.05$ vs. isotype/vehicle; one-way ANOVA).
- C Recruitment of neutrophils (N) and classical monocytes (cMOs) to the peritoneal cavity of WT mice treated with recombinant murine uPA-PAI-1, recombinant human uPA-recombinant murine PAI-1 heteromers, recombinant murine DFP-uPA-PAI-1, or vehicle (mean \pm SEM for $n = 4-6$ mice per group; $^{\#}P < 0.05$ vs. saline; one-way ANOVA).

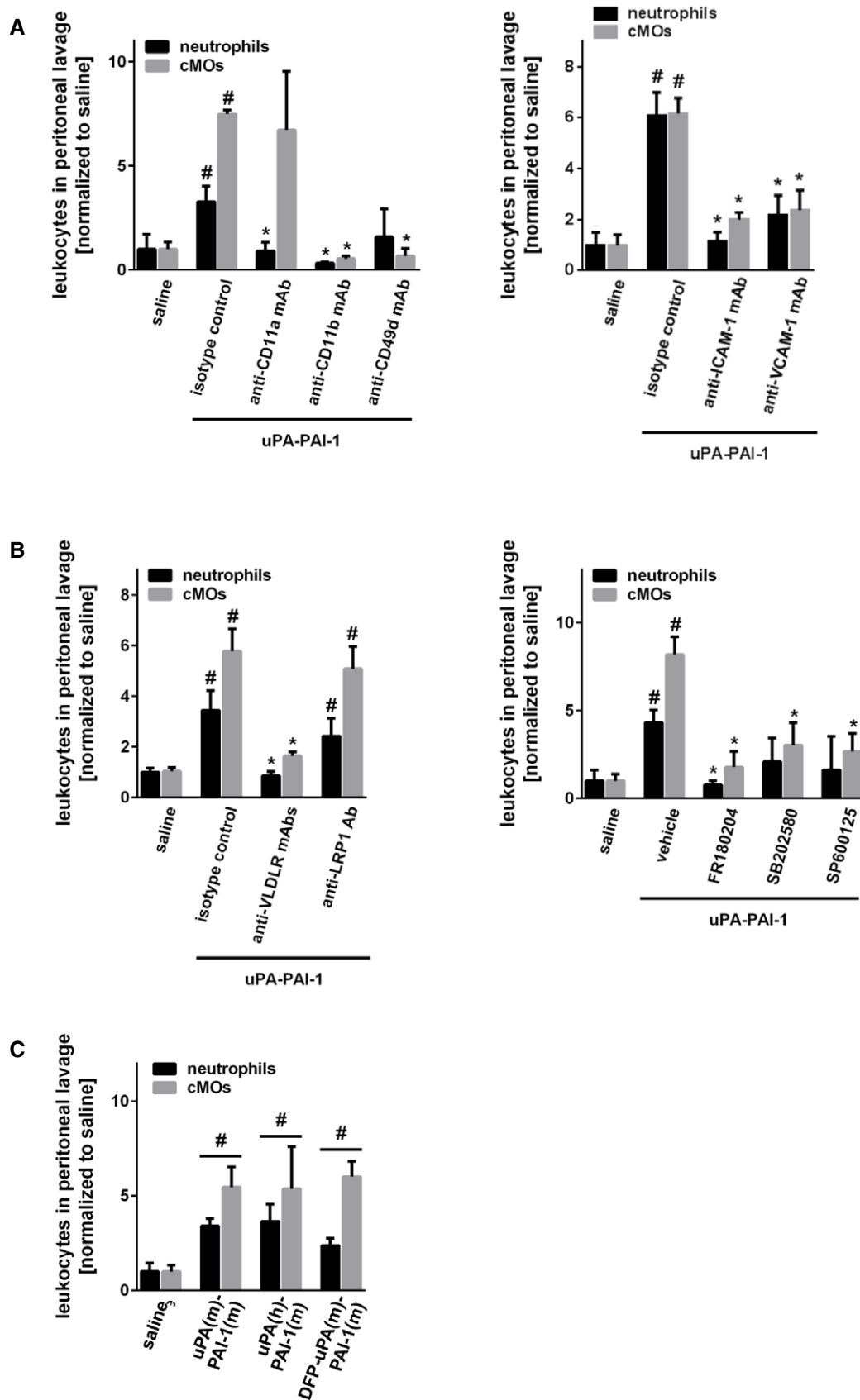


Figure EV2.

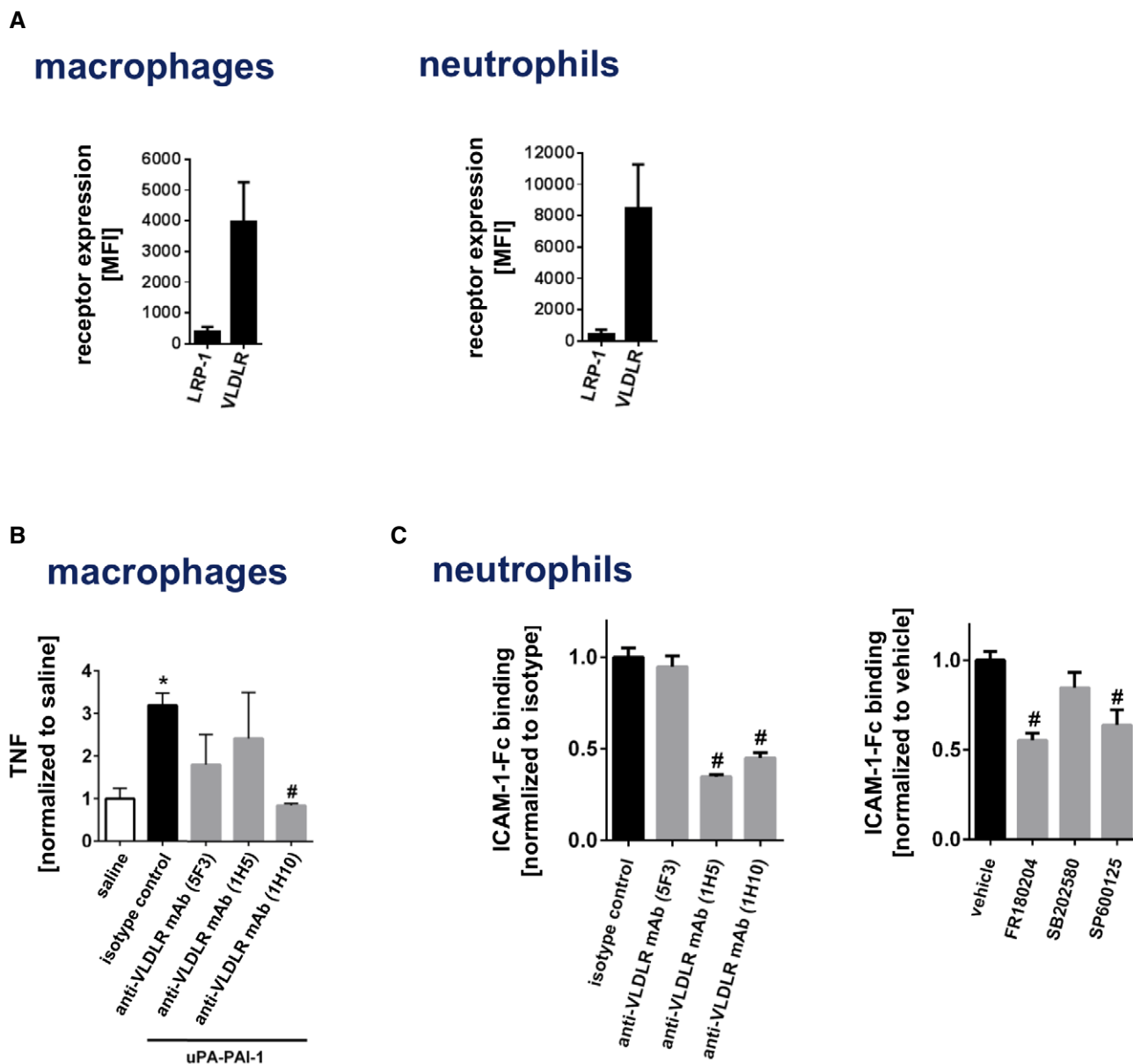


Figure EV3. Molecular mechanisms underlying uPA-PAI-1-dependent responses of macrophages and neutrophils.

- A Surface expression of LRP-1 or VLDLR on mouse RAW macrophages or bEnd.3 endothelial cells (mean \pm SEM for $n = 3$ experiments per group).
- B Production of TNF by mouse RAW macrophages upon exposure to blocking antibodies directed against different epitopes of VLDLR as assessed by multi-channel flow cytometry (mean \pm SEM for $n = 4-6$ experiments per group; * $P < 0.05$ vs. saline; # $P < 0.05$ vs. isotype control; one-way ANOVA).
- C Binding of recombinant murine ICAM-1/CD54-Fc to blood neutrophils from WT mice upon exposure to blocking antibodies directed against different epitopes of VLDLR or the MAPK inhibitors FR180204 (ERK), SB202580 (p38), or SP600125 (JNK) as assessed by flow cytometry (mean \pm SEM for $n = 4-6$ mice per group; # $P < 0.05$ vs. isotype control/vehicle; one-way ANOVA).

Figure EV4. Correlation of neutrophil infiltration and uPA/PAI-1 expression in human breast cancer samples.

- A, B Correlation of uPA or PAI-1 protein expression (ELISA) and neutrophil infiltration (histochemistry and light microscopy) in human breast cancer samples, representative images (A; histological grades: G1-3; scale bar: 100 μ m) and quantitative data (B; histological grades: G2 or G3; $n = 10-29$ samples per group).

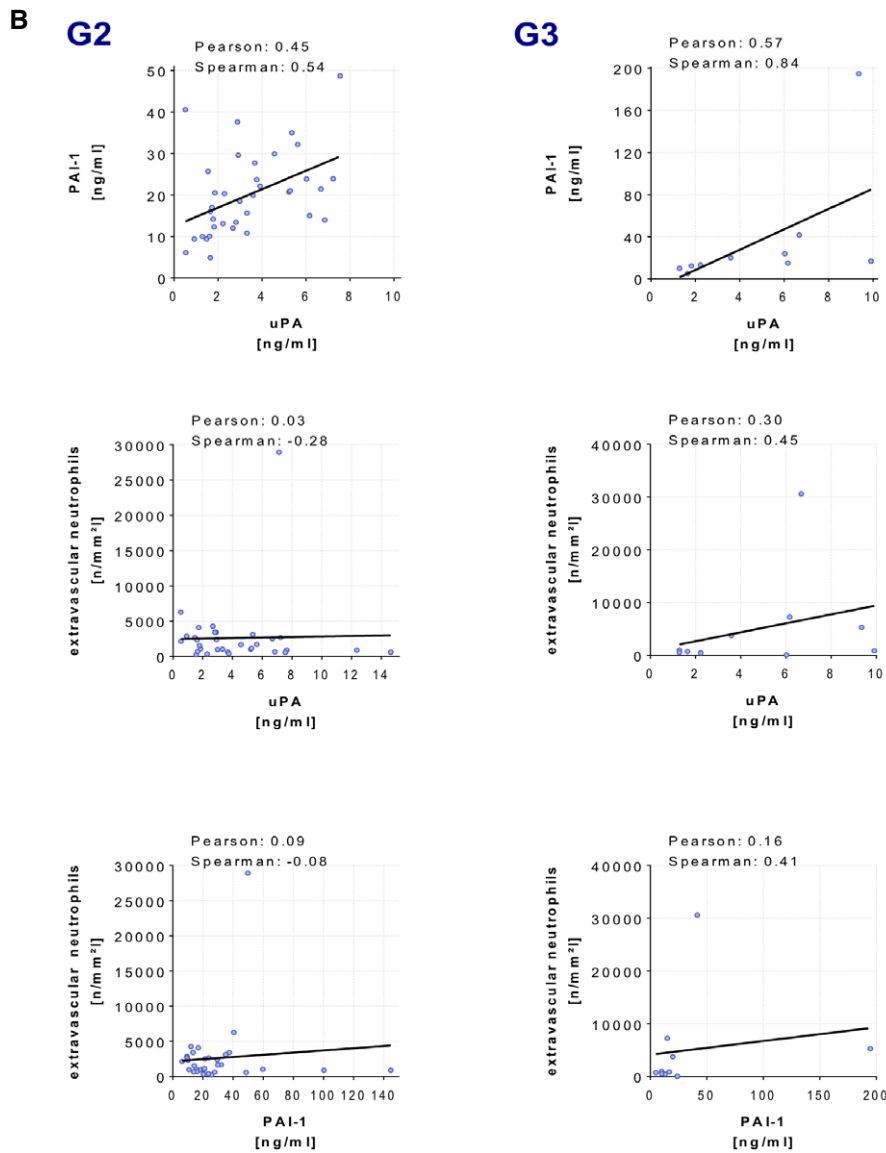
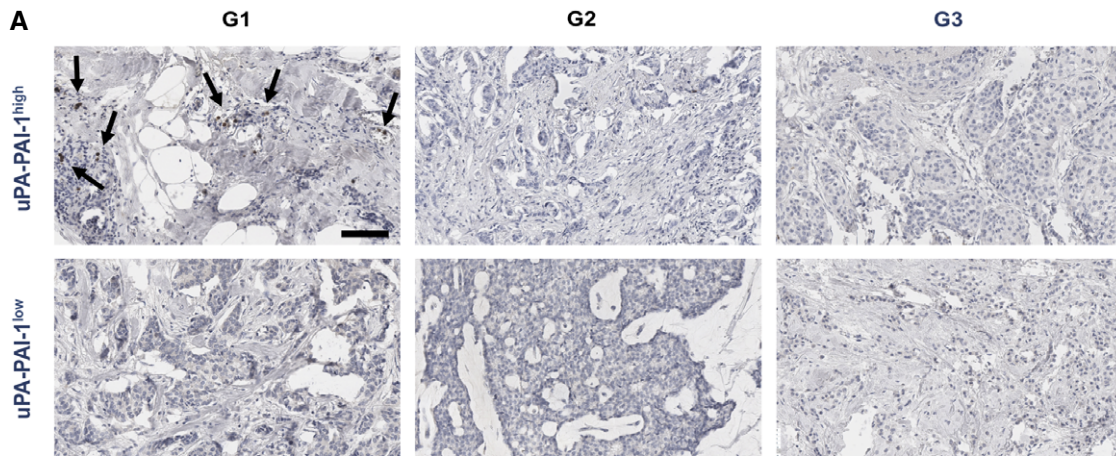


Figure EV4.

Figure EV5. Overall survival of breast cancer patients of the METABRIC cohort with respect to disease stage.

- A Composition of analyzed patients of the METABRIC cohort with respect to the disease stage.
- B Overall survival of PLAU-SERPINE1^{low} and PLAU-SERPINE1^{high} breast cancer patients in all disease stages (0–4) and advanced stages (2–4).
- C Mosaic plot depicting cross-tabulation and chi-squared analysis between high RNA expression of PLAU or SERPINE1 in the tumor and the molecular breast cancer subtype as defined by the 3-gene-classifier.

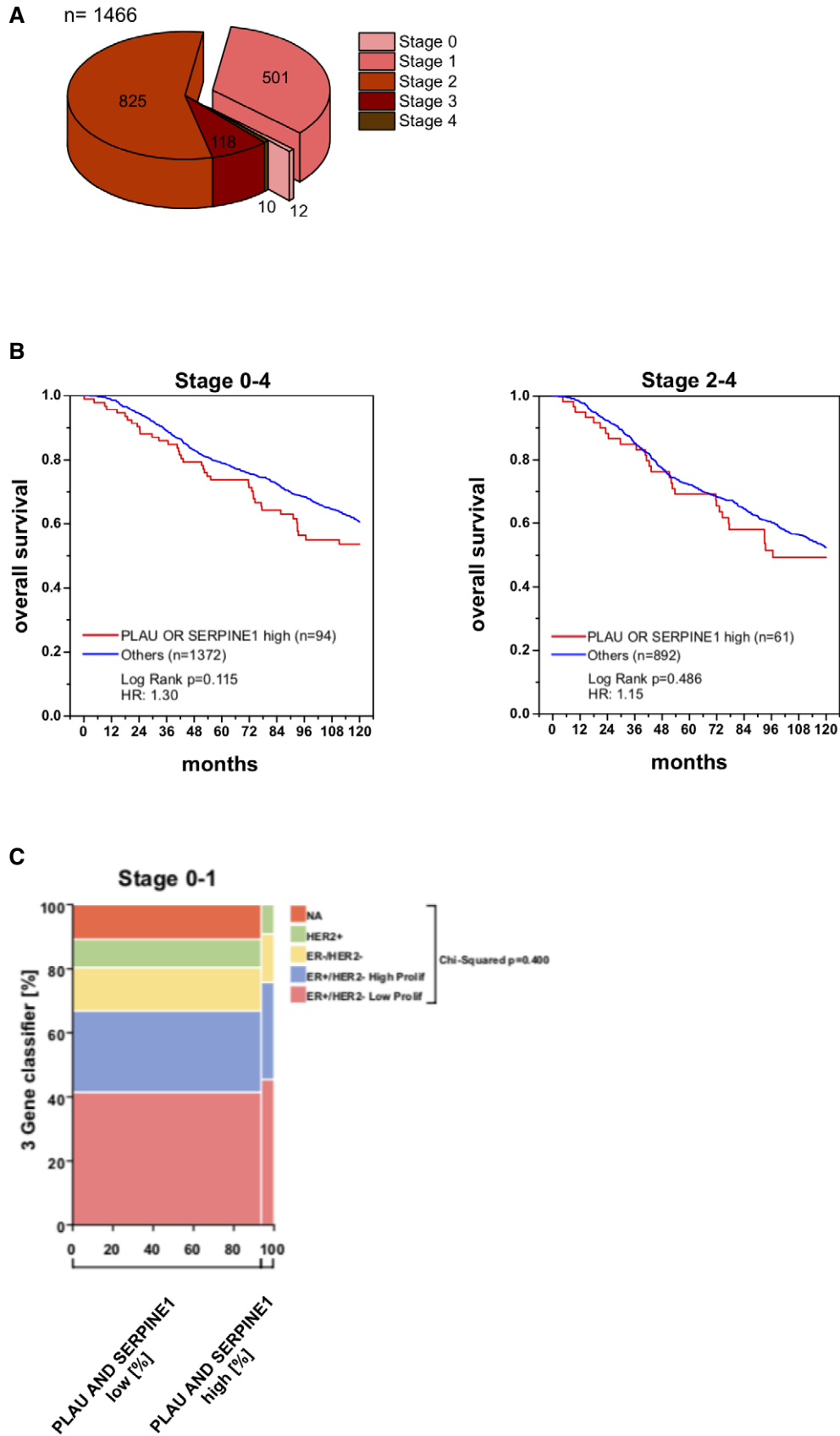


Figure EV5.